DOI 10.1007/s10553-018-0884-0
Chemistry and Technology of Fuels and Oils, Vol. 53, No. 6, January 2018 (Russian Original No.6, November – December, 2017)

NUMERICAL SIMULATION OF HYDRAULIC FRACTURING IN WEAKLY CONSOLIDATED SANDSTONE

Baitao Fan[1,2], Jingen Deng[1], Hai Lin[2], Wei Liu[1], and Quiang Tan[1]

The article presents a detailed finite-element model for investigating hydraulic fracture propagation in weakly consolidated sandstone. Elastoplastic deformation of the rock matrix, pore fluid flow, initiation and propagation of hydraulic fractures as well as flow of fracturing fluid within a fracture and leakoff into the formation are considered interdependently. The extended Cam-Clay model is used to achieve a more precise assessment of the mechanical behavior of weakly consolidated sandstone. Parametric studies are performed to investigate the effect of the fracturing parameters on the fracture patterns. The numerical results show that extremely short and narrow fractures are formed if low-efficiency fracturing fluid is used to initiate fractures in weakly consolidated sandstone with a zone of shear dilation formed on both faces of the fracture. In contrast, longer and wider fractures initiation of which is desirable in frac-pack (hydraulic fracturing) operations with the use of proppant may be obtained with the use of high- efficiency fracturing fluid and more compact zones are created near the fracture. However, the structure of the compaction zone produces an insignificant decrease in permeability. It is also shown that plastic deformation of the rock matrix has a significant impact on the geometry of a fracture, and this must be taken into account in the design of frac-pack operations with the use of proppant in weakly consolidated sandstone reservoirs.

---

[1]State Key Laboratory of Petroleum Resources and Engineering, China University of Petroleum, Beijing, China. [2]State Key Laboratory Offshore Oil Exploitation, CNOOC China Limited, Tianjin Branch, China. *E-mail: dengjingen@126.com.*Translated from *Khimiya i Tekhnologiya Topliv i Masel*, No. 6, pp. 85 – 92, November – December, 2017..

Key words: *weakly consolidated sandstone, frac-pack treatment of a formation with the use of proppant, hydraulic fracturing, fracture propagation, shear dilation, compaction, numerical simulation.*

In the past several dozen years hydraulic fracturing (frac-pack treatment) of oil reservoirs with the use of proppant has been widely used to complete weakly consolidated offshore sandstone reservoirs, since the technique can achieve sand control and at the same time improve production [1]. The most important step to successful frac-pack treatment of oil reservoirs with the use of proppant is to form short, but wide planar fractures which are subsequently packed with proppant and which provide a high degree of conductivity during the production stage. However, in view of the complex mechanical behavior of unconsolidated sandstone and the high degree of permeability, initiation and propagation of fractures in weakly consolidated sandstone are less understood than is propagation of fractures in hard rock, which imposes a host of constraints in the design of frac-pack operations with the use of proppant.

Laboratory experiments [2–5] have been carried out to investigate the mechanism of hydraulic fracturing in weakly consolidated sandstone. The results demonstrate that diffusion of pore pressure ahead of the fracture tip results in plastic deformation and shear failure as a consequence of shearing forces which is also a cause of subsequent fracture propagation. It has also been shown that the properties of the fracturing fluid

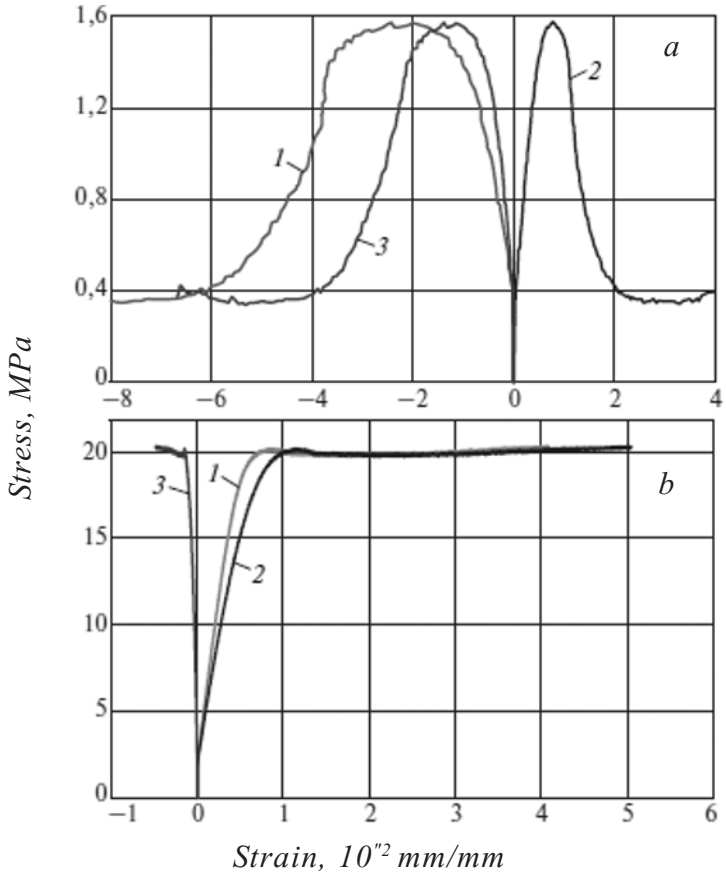

Fig. 1. Stress-strain curves of (a) uniaxial compression and (*b*) triaxial compression in weakly consolidated sandstone: *1*, *2*, *3* – volumetric, axial, and radial strain, respectively.

have a significant effect on fracture propagation in weakly consolidated sandstone. As a rule, clear planar fractures are formed with the use of high-efficiency fracturing fluid with low filtrate leakoff, whereas branching fractures are likely to be produced if low-efficiency fracturing fluid with high filtrate leakoff is used.

It is obvious from the experimental data that hydraulic fracturing in weakly consolidated sandstone differs from hydraulic fracturing in more highly consolidated sandstone and, thus, the conventional hydraulic fracturing model based on the linear mechanics of fracture initiation is not applicable for modeling fracture propagation in weakly consolidated sandstone. The initiation and propagation of hydraulic fractures in weakly consolidated sandstone are investigated in [6] using damage mechanics based on the method of finite elements, and it is found that oriented perforation is beneficial for producing simple planar fractures, initiation of which is desirable for frac-pack treatment with the use of proppant. In [7] a fracture in weakly consolidated oil-bearing sandstones is investigated as a zone of shear dilation with high permeability and not as discrete fractures, the 3D model of a finite elastoplastic element for modeling the propagation of this zone of shear dilation is improved, and a model of pressure variation in the course of the operation is modified. In [8] it is suggested that shear failure is the principal mechanism in hydraulic fracturing in weakly consolidated sandstone as a result of an oriented high-permeability zone instead of simple planar fractures, and the influence of anisotropy of in-situ stresses on fracture propagation in hydraulic fracturing in weakly consolidated sandstone is investigated. Both shear failure and tensile failure in the course of hydraulic fracturing in weakly consolidated sandstone is considered in [9, 10], and the initiation and propagation of the failure zone is investigated in the case of tension with the use of the cohesive zone model. The results led to the understanding that hydraulic fracturing in weakly consolidated sandstone is accompanied by plastic deformation along the fractures and relatively high net pressure at the opening of a fracture in hydraulic fracturing. Possible plastic compression of weakly consolidated sandstone is studied in [11] and a numerical model for simulating hydraulic fracturing is developed, in which the mechanical behavior of weakly consolidated sandstone is characterized by the modified Cam-Clay model.

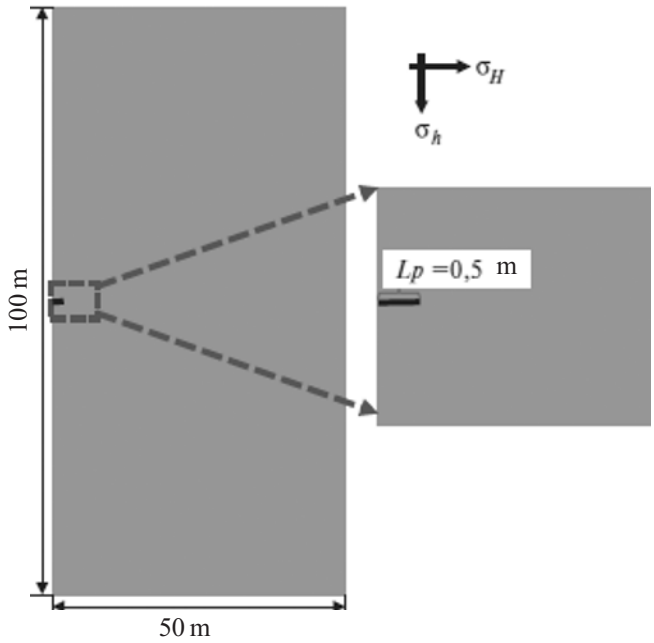

Fig. 2. Geometry and mesh of model of hydraulic fracturing in weakly consolidated sandstone.

Despite the above experimental and numerical studies, the mechanism underlying the initiation and propagation of fractures in weakly consolidated sandstone needs to be studied in greater detail. Therefore, in the present investigation we develop a detailed finite-element model that takes into account both elastoplastic deformation of the rock matrix, pore fluid flow, and initiation and propagation of fractures as well as fracturing fluid flow within the fracture and leakoff into the formation. Using this model, typical initiation of fractures in consolidated sandstone is predicted and the influence of the properties and rate of injection of the hydraulic fracturing fluid on fracture initiation and propagation is studied.

Investigations of uniaxial and triaxial shear were performed on rock cores extracted from a typical weakly consolidated sandstone formation in the Bohai field (China). The results are presented in Fig. 1. It is apparent that the uniaxial compressive strength is low, generally not higher than 2 MPa. It may also be seen that weakly consolidated sandstone possesses distinctive features in the form of shear tension and strain softening under uniaxial compression and shear compression under high confining pressure. It is obvious from the experiments that in the course of hydraulic fracturing weakly consolidated sandstone around fractures experience stresses directed along different paths under different conditions [2] and, consequently, both shear tension and shear compression are encountered. Therefore, we used the modified Cam-Clay model to achieve a more precise description of the behavior of weakly consolidated sandstone with the yield function in the form

$$\frac{q^2}{p'^2} + M\left(1 - \frac{p'_0}{p'}\right) = 0 \tag{1}$$

where $p2$ is the effective mean stress; q, effective equivalent shear stress; M, slope of critical state line, which may be obtained from the internal friction angle; and $p_0 2$, preconsolidation pressure.

Weakly consolidated sandstone is usually distinguished by a high permeability and significant leakage of the fracturing fluid from the fracture into the formation, which evolves into a change in the pore pressure and the effective stress and, consequently, a change in the porosity and permeability. From this observation it follows that the variation in the pore pressure and in the elastoplastic deformation are coupled phenomena. In the present article the theory of elastoplastic deformation is used to describe the process. The stress equilibrium equation is given as follows:

$$\sigma_{ij,j} + f_i = 0 \tag{2}$$

where f_i is the body force per unit volume and y_{ij} the total stress, which is related to the effective stress by the equation $\sigma_{ij} = \sigma'_{ij} - \alpha p_p \delta_{ij}$ (p_p is the pore fluid pressure and δ_{ij} the Kronecker delta).

Biot's coefficient a is assumed to be 1 in view of the high porosity of weakly consolidated sandstone. The strain-displacement relationship is expressed by the formula

$$\varepsilon_{ij} = \frac{1}{2}\left(u_{i,j} + u_{j,i}\right) \tag{3}$$

where ε_{ij} is deformation and u_i displacement.

The basic equation of pore fluid drainage may be obtained from Darcy's law and the law of conservation

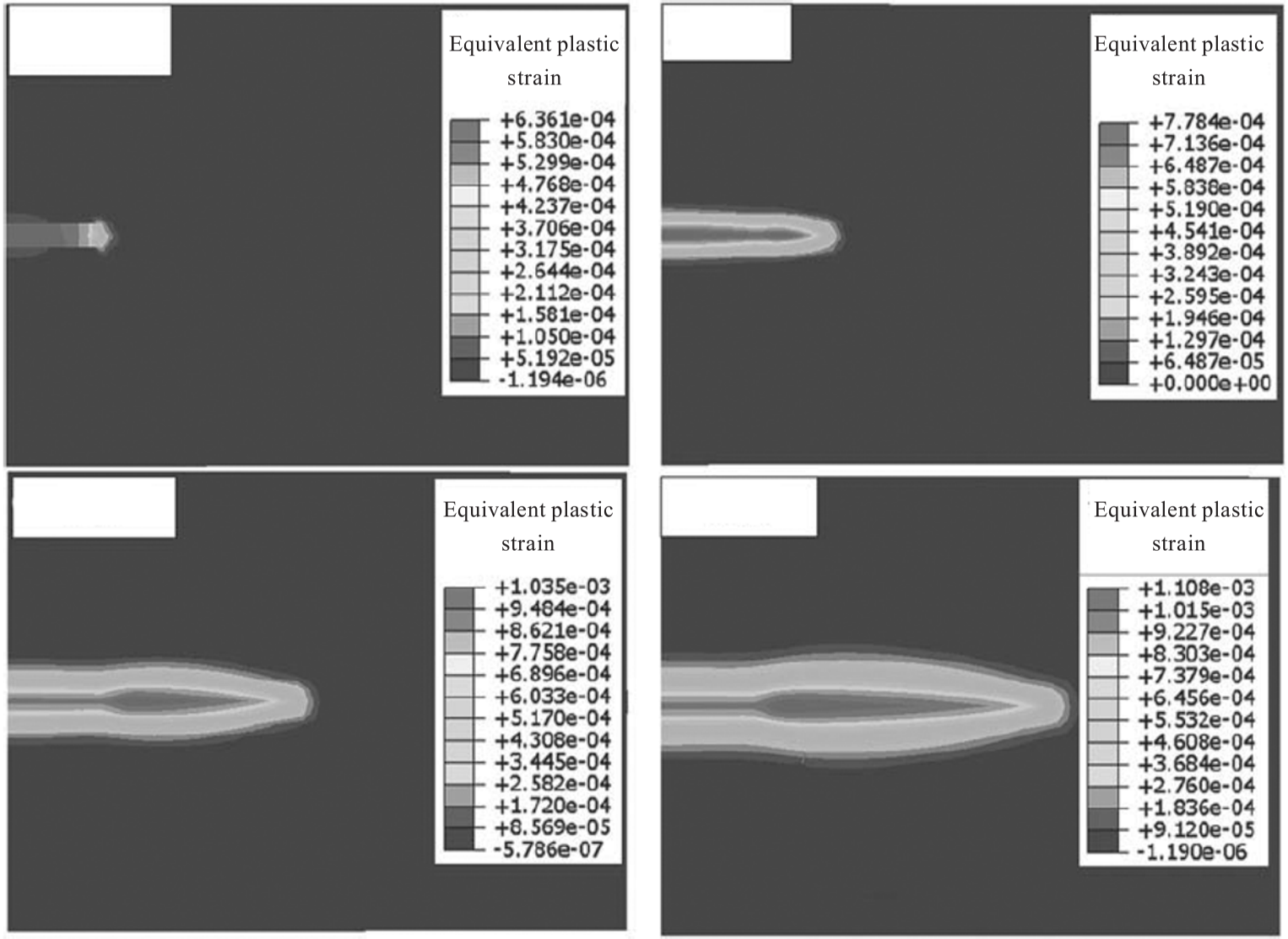

Fig. 3. Hydraulic fracture in shear dilation zone at different time instants (low-efficiency fracturing fluid).

of fluid mass and is written as

$$\varepsilon_v - (k/\mu)p_{p,ii} = 0 \tag{4}$$

where ε_v is volumetric strain; k, permeability; and μ, dynamic viscosity.

A decrease in permeability as a result of shear compaction is described by what is known as the Kozeny–Carmen ratio,

$$\frac{k}{k_0} = \left[\frac{1}{\phi_0} e^{\varepsilon_v^{\frac{2}{3}}} + \frac{\phi_0 - 1}{\phi_0} e^{\varepsilon_v^{-\frac{1}{3}}}\right]^3 \tag{5}$$

where k_0 is the initial permeability and ϕ_0 the initial porosity.

Shear dilation indicates that micro-fractures have formed within the rock mass and that permeability could grow significantly. From the data of [12], permeability grows as a result of shear dilation, as described by the equation

$$k = \frac{V\varepsilon_v^2}{48} \tag{6}$$

where V is the volume of the element used in the finite-element simulation.

In the present study initiation and propagation of fractures in weakly consolidated sandstone is modeled by the cohesive zone method. By assuming the existence of a zone of fracture initiation ahead of the fracture tip, the method is able to replace the physically meaningless singularity of linear elastic fracture mechanics at the fracture tip. The criterion of fracture initiation in the cohesive zone method may be expressed as follows:

$$\left\{\frac{\langle \sigma_n \rangle}{\hat{\sigma}_n}\right\}^2 + \left\{\frac{\tau_s}{\hat{\tau}_s}\right\}^2 + \left\{\frac{\tau_t}{\hat{\tau}_t}\right\}^2 \geq 1 \tag{7}$$

where σ_n, τ_s, and τ_t are the normal cohesive stress and the two shear cohesive stress components, respectively, and $\hat{\sigma}_n, \hat{\tau}_s$ *and* $\hat{\tau}_t$ the corresponding values of the cohesive strength. Following initiation, propagation of a fracture obeys a law of damage evolution of the form

$$\left\{\frac{G_n}{G_{nC}}\right\}^2 + \left\{\frac{G_s}{G_{sC}}\right\}^2 + \left\{\frac{G_t}{G_{tC}}\right\}^2 \geq 1 \tag{8}$$

where G_n, G_s, and G_t are the fracture energies dissipated in the normal and two shear directions, respectively, while G_{nC}, G_{sC}, and G_{tC} are the corresponding critical fracture energies.

The basic equation for fluid flow within a fracture may be obtained by combining the equation of lubrication and law of conservation of fluid mass:

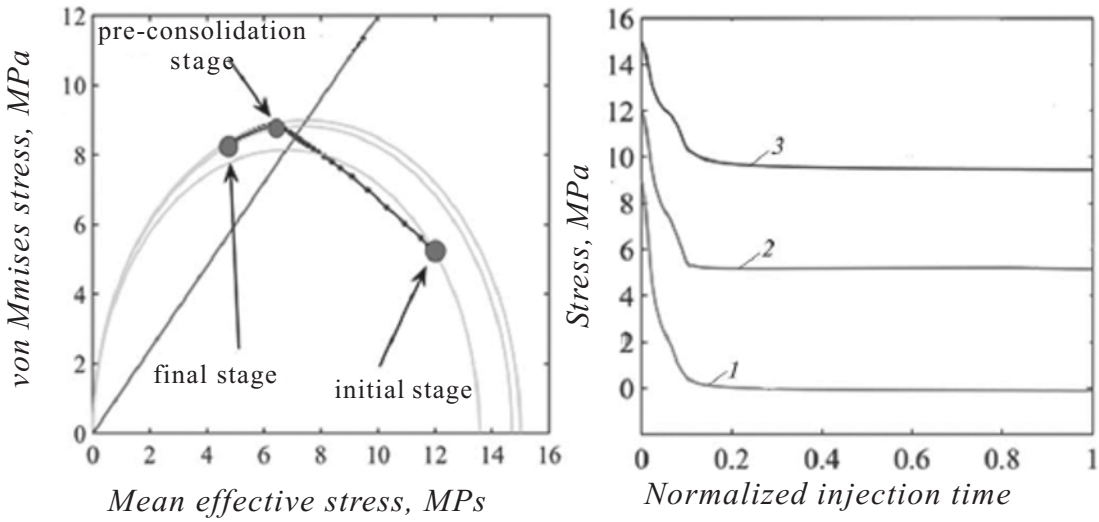

Fig. 4. Typical stress path (*a*) and effective principal stress (*b*) (low-efficiency fracturing fluid): *1*, *2*, *3*: minimum, middle, and maximum principal stress.

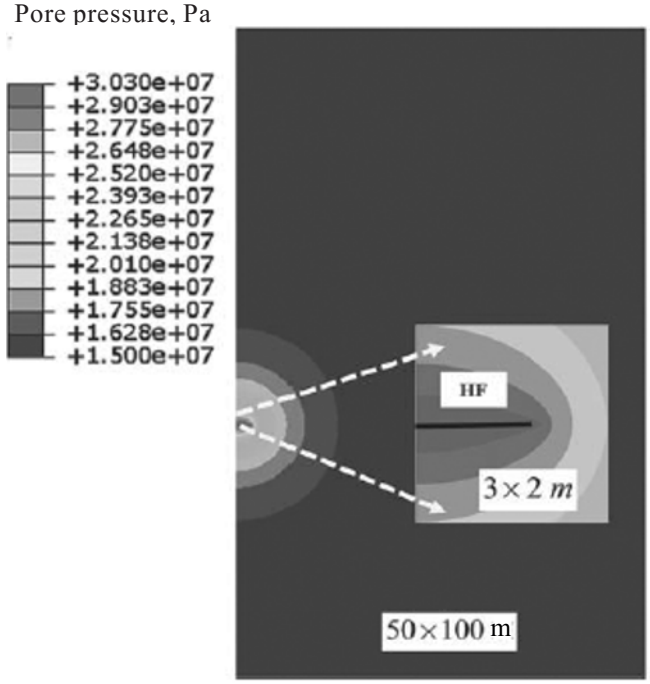

Fig. 5. Distribution of pore pressure near fracture tip (low-efficiency fracturing fluid) .

$$\frac{\partial w}{\partial t} - \frac{1}{12\mu}\nabla\left(w^3\nabla p\right) + \left(q_t + q_b\right) = 0 \tag{9}$$

where w is the fracture opening; p, fluid pressure within the fracture; and q and q_b, leakoff rates on the two fracture faces, which may be described thus:

$$q_t = c_t\left(p - p_t\right) \qquad q_b = c_b\left(p - p_b\right) \tag{10}$$

where c_t and c_b are the leakoff coefficients on each of the two faces of the fracture and p_t and p_b the pore

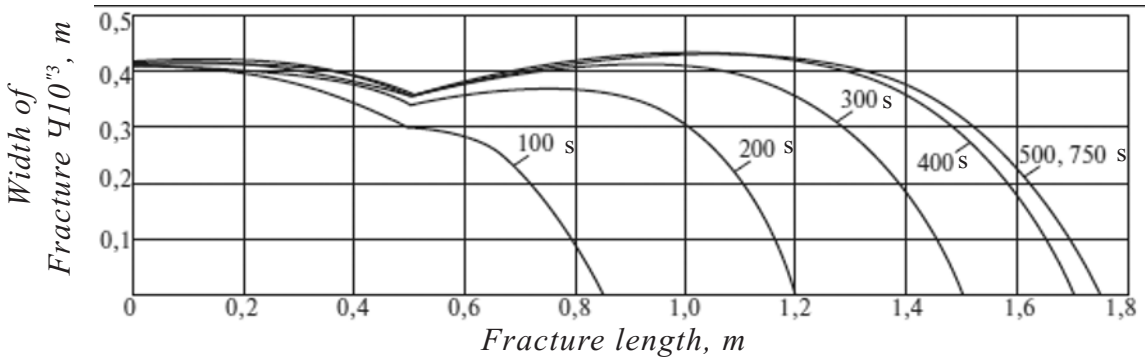

Fig. 6. Width of fracture initiated by low-efficiency fracturing fluid at different time instants (cf. digits next to curves).

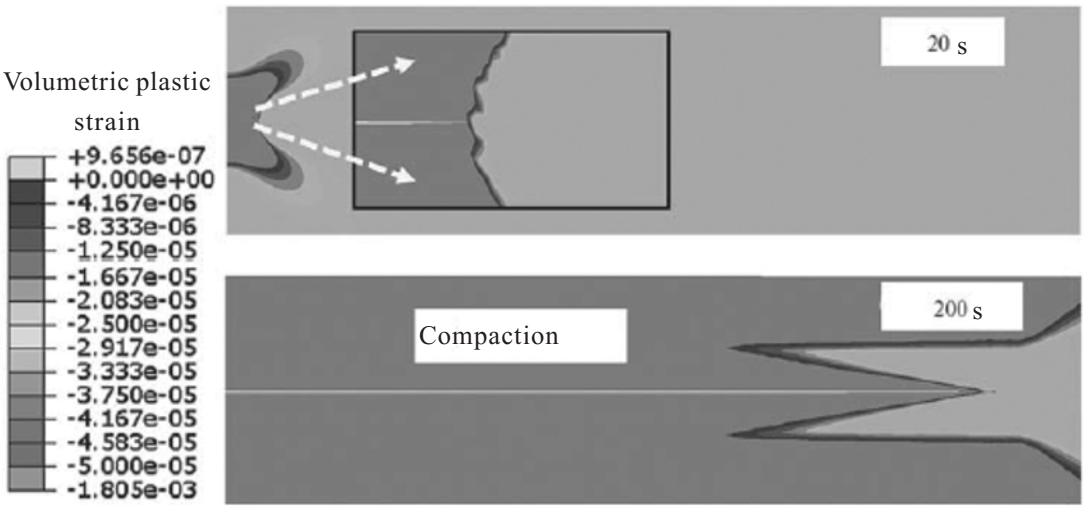

Fig. 7. Hydraulic fracture and compaction zone (high-efficiency fracturing fluid).

pressures on the two faces.

The above coupled elastoplastic model is solved by the finite-element method with the use of the general-purpose ABAQUS program package for nonlinear calculations. Simulation with the use of the above parameters for a typical weakly consolidated sandstone reservoir in the Bohai oil field in China was performed to investigate the mechanisms of hydraulic fracturing in weakly consolidated sandstone and the influence of the properties of the fracturing fluid on the fracture geometry.

The geometry and mesh of the model are presented in Fig. 2. In view of the symmetry of the problem, only half the model is created. The model is 50 m long along the horizontal axis and 100 m wide along the vertical axis. The mesh in the middle of the model is refined and the size of the zone with the refined mesh is 50 m long and 4 m wide. Zero-thickness pore pressure cohesive elements are inserted into the middle of the model along the horizontal axis. The first several cohesive elements on the left side are assigned zero cohesive strength and an initial opening to model the perforation. The top, bottom, and right sides of the model are fixed, while symmetry conditions are enforced on the left side. The input parameters used in the simulations are presented below.

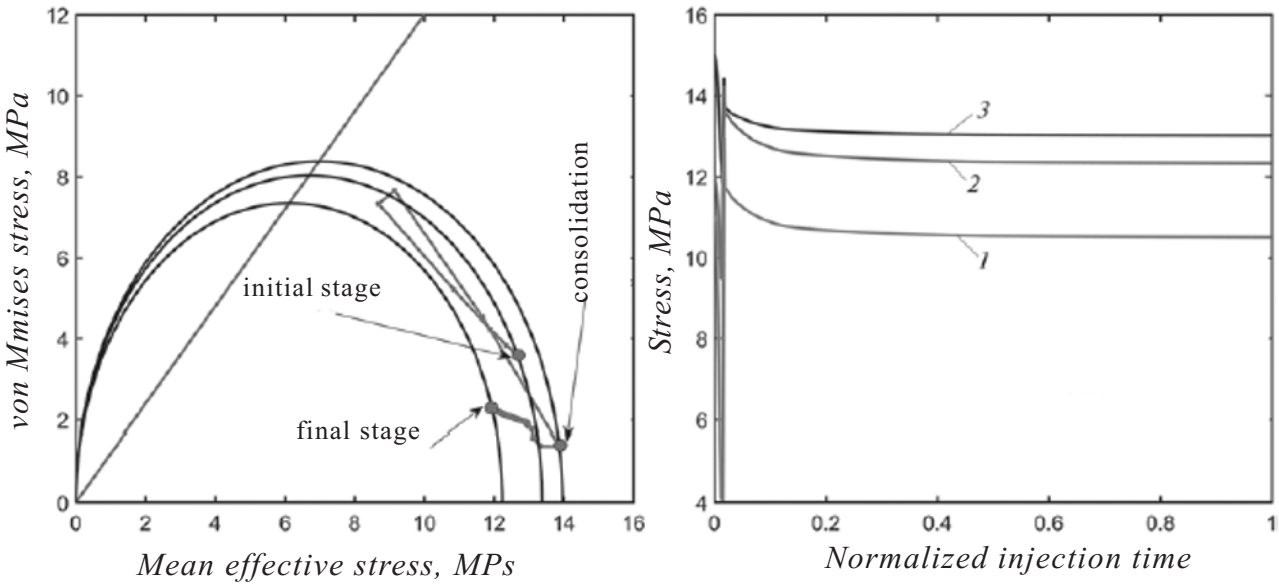

Fig. 8. Typical stress path (*a*) and effective principal stresses (*b*) (high-efficiency fracturing fluid): *1*, *2*, *3*: minimum, middle, and maximum principal stress.

Slope of normal consolidation line 0.1
Slope of unloading–reloading line 0.2
Slope of critical state line 1.2
Poisson's ratio 0.27
Overconsolidation ratio 1,18
Tensile strength, MPa 0.01
Critical fracture energy, J/m^2 10
in-situ stresses y_v/y_H /y_h, MPa 30/27/24
Pore pressure, MPa 15
Porosity 0.3
Permeability, mD 500
Dynamic viscosity, mPa " s 10
Perforation depth, m 0.5
Injection rate per unit thickness, m^3/s/m 0.001
Well injectivity with use of fracturing fluid, m/s/Pa
low-efficiency fracturing fluid 1.0e-8
high-efficiency fracturing fluid 1.0e-11

The data of Fig. 3 are the results of propagation of a hydraulic fracture at four different time instants under the effect of low-efficiency fracturing fluid. Weakly consolidated sandstone usually exhibits high permeability, while low-efficiency fracturing fluid tends to leak off from the fracture into the formation. The data of the figure indicate that the fracture is initiated and propagates in the direction of maximum in-situ stress. However, due to the significant filtrate leakoff, the fracture is very short. Following injection lasting 500 s, the fracture does not propagate any further and its final length is only 1.9 m. Note, too, that a fracture produced with injection of low-efficiency fracturing fluid is accompanied by a shear dilation zone near the two

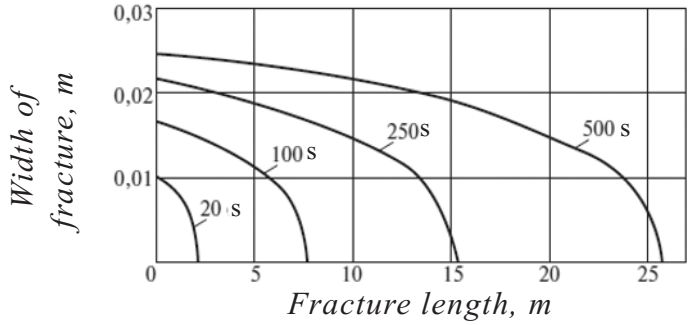

Fig. 9. Width of fracture initiated by high-efficiency fracturing fluid at different time instants (cf. digits next to curves).

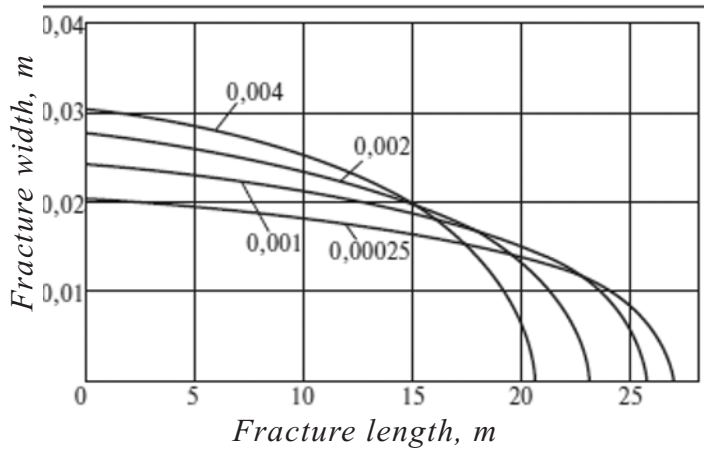

Fig. 10. Width of fracture initiated by high-efficiency fracturing fluid at different injection rates ($m^3/s/m$; cf. digits next to curves).

fracture faces.

A typical stress path experienced by points on the stress line is presented in Fig. 4. It is apparent that the significant leakoff of fracturing fluid into the zone ahead of the fracture tip and the growth in the pore together lead to an increase in the deviatoric pressure and a decrease in the mean stress (Fig. 5) and, consequently, shear failure occurs with dilation. Permeability increases ahead of the fracture tip due to shear dilation, leading to further growth in pore pressure, which causes tensile failure of the zone ahead of the fracture tip and, consequently, further propagation of the fracture.

The width of the fracture at different time instants is shown in Fig. 6 and indicates that fractures initiated by low-efficiency fracturing fluid are extremely narrow. This is because pore pressure in the neighborhood of a fracture is high due to the high volume of leakoff of fluid into the rock mass and, consequently, the effective net pressure is low.

Experiments clearly demonstrated that increasing the viscosity of the fracturing fluid or adding leakoff control components or low-permeability filtercake building additives in the course of hydraulic fracturing in weakly consolidated sandstone could reduce filtrate leakoff and increase the efficiency of the fracturing fluid. The propagation of a hydraulic fracture induced by high-efficiency fracturing fluid is shown in Fig. 7. It is evident that the fracture is initiated and propagates in the direction of maximum principal pressure. It should

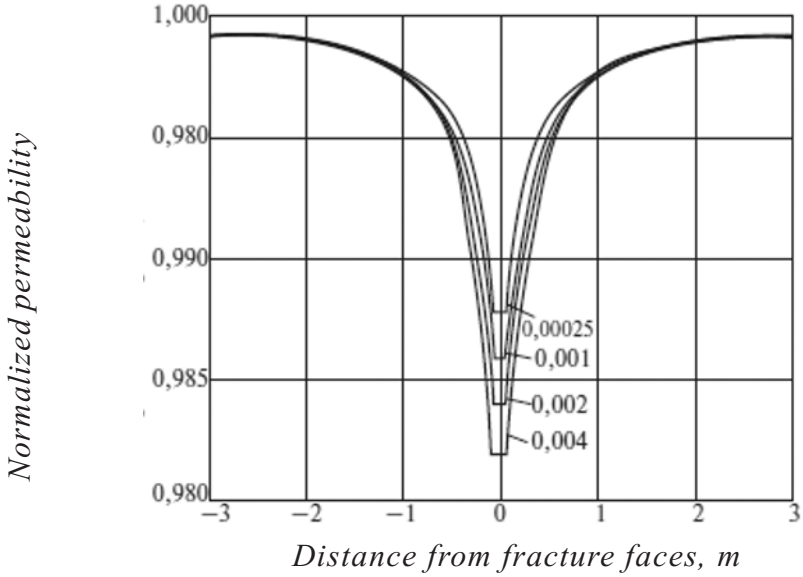

Fig. 11. Permeability as a function of distance from faces of fractures initiated by high-efficiency fracturing fluid at different injection rates ($m^3/s/m$; cf. digits next to curves).

also be noted that the slight compaction zone around the fracture is initiated under the effect of the high-efficiency fracturing fluid, which differs from the shear dilation zone produced with the use of low-efficiency fracturing fluid.

The stress path experienced by points on the damage path (fracture trajectory) over the course of the entire hydraulic fracturing treatment is shown in Fig. 8. Leakoff of high-efficiency fracturing fluid into the zone ahead of the fracture tip is limited and the variation of the pore pressure insignificant. The rock experiences slight compaction until the stress exceeds the pre-consolidation stress.

The width and length of a fracture at different time instants are shown in Fig. 9. It is evident that the fracture width is on the order of 2–3 cm and that its final length is 25 m.

From the results of the experiments it may be concluded that the injection rate of the fracturing fluid exerts a strong influence on the propagation of hydraulic fractures. A better understanding of this influence will be useful for optimization of the process of hydraulic fracturing. The profiles of fractures in weakly consolidated sandstone in which the same total volume of high-efficiency fracturing fluid was injected but at different injection rates are shown in Fig. 10. The figure shows that the width of the fracture grows with increasing injection rate, while its length decreases. Variations in permeability as a function of distance from the fracture face following hydraulic fracturing are presented in Fig. 11. It is apparent that due to injection of high-efficiency fracturing fluid the compaction zone induces a decrease in permeability near the fracture faces. However, the decrease in permeability is quite moderate, with maximum reduction only 1–2% of the initial permeability, with rapid recovery of the initial level at a distance from the fracture faces. Consequently, the influence of compaction on subsequent production induced by injection of high-efficiency fracturing fluid is not significant.

Thus, the coupled poro-elastoplastic numerical model for investigating the mechanism of hydraulic fracturing in weakly consolidated sandstone has been improved in the present work and the influence of the action of the properties of the fracturing fluid on the behavior of hydraulic fracturing has been studied. The following conclusions may be reached on the basis of the investigations.

Weakly consolidated sandstone considered in the present article exhibits shear dilation in the course of tests under uniaxial compression conditions and shear compression under high confining pressure

conditions. Both of behaviors may be present in the course of hydraulic fracturing in weakly consolidated sandstone, consequently, a model capable of describing both types of behavior should be used in modeling.

Hydraulic fracturing in weakly consolidated sandstone with low-efficiency hydraulic fracturing fluid leads to extremely short and narrow hydraulic fractures accompanied by shear dilation zones around the fractures faces. It is possible that such narrow fractures cannot be maintained, leading to low efficiency of hydraulic fracturing with the use of proppant.

Increasing the viscosity or adding to the fracturing fluid of components to effectively reduce filtrate leakoff may significantly increase the efficiency of the hydraulic fracturing fluid and initiate short, though wide fractures, which are desirable by the frac-pack with the use of proppant. Certain zones of slight compaction will be initiated near the fracture faces. However, the reduction in permeability caused by such compaction may prove to be slight.

An increase in the rate of injection of high-efficiency hydraulic fracturing fluid leads to an increase in the fracture width and a decrease in its length.

The authors wish to acknowledge the financial support provided by the National Science and Technology Major Project (No. 2016ZX05058-002-006).

REFERENCES

1. J. Ayoub, J. Kirksey, B. Malone, et al., Hydraulic fracturing of soft formations in the gulf coast, in: *SPE Formation Damage Control Symposium*, Lafeyette, Illinois, USA, Feburary 26–27, 1992; SPE 23805

2. M. Khodaverdian and P. McElfresh, Hydraulic fracturing stimulation in poorly consolidated sand: mechanisms and consequences, in *SPE Annual Technical Conf.,* Dallas, Texas*,* USA, October 1–4, 2000; SPE63233

3. H. Jasarevic, E. Golovin, A. Chudnovsky, et al., Observation and modeling of hydraulic fracture initiation in cohesiveless sand, in: *44th US Rock Mechanics Symposium and 5th US–Canada Rock Mechanics Symposium*, Salt Lake City, Utah, USA, June 27–30, 2010; ARMA 10-360

4. C. J. de Pater and Y. Dong, Experimental study of hydraulic fracturing in sand as a function of stress and fluid rheology, in: *SPE Hydraulic Fracturing Technology Conference,* College Station, Texas, USA, January 29–31, 2007; SPE105620

5. L. N. Germanovich, R. S. Hurt, J. A. Ayoub, et al., Experimental study of hydraulic fracturing in unconsolidated materials, in: *SPE International Symposium and Exhibition on Formation Damage Control*, Lafayette, Louisiana, USA, February 15–17, 2012; SPE151827

6. J. Deng, J. Wang and J. Yan, Study on propagation law of hydraulic fractures of gas pool in unconsolidated sandstone, *Rock and Soil Mechanics*, 23, No. 1, 72–74 (2002).

7. B. Xu and R. C. Wong, A 3D finite element model for history matching hydraulic fracturing in unconsolidated sands formation, *Journal of Canadian Petroleum Technology*, 49, No. 4, 58–66 (2010).

8. Z. Zhai and M. M. Sharma, A new approach to modeling hydraulic fractures in unconsolidated sands, in: *SPE Annual Technical Conference and Exhibition*, Dallas, Texas, USA, October 9–12, 2005; SPE96246

9. P. Papanastasiou, The influence of plasticity in hydraulic fracturing, *International Journal of Fracture*, 84, No. 1, 61–79 (1997).

10. D. Lee and M. M. Sharma, A fully-coupled, poro-elasto-plastic, 3-D model for frac-pack treatments in poorly consolidated sands, in: *SPE Hydraulic Fracturing Technology Conference and Exhibition*, The Woodlands, Texas, USA, January 24–26; SPE184847
11. A. Abou-Sayed, K. Zaki, G. Wang, et al., Fracture propagation and formation disturbance during injection and Frac-Pack operations in soft compacting rocks, in: *SPE Annual Technical Conference and Exhibition*, Houston, Texas, USA, September 26–29, 2004; SPE90656
12. S. Yuan and J. Harrison, Propagation of a hydro-mechanical local degradation approach and its application to modelling fluid flow during progressive fracturing of heterogeneous rocks." *International Journal of Rock Mechanics and Mining Sciences*, 42, No. 7, 961–984 (2005)